

## Using controlled-source electromagnetic (CSEM) for CO<sub>2</sub> storage monitoring in the North Dakota CarbonSAFE project

César Barajas-Olalde<sup>1</sup>, Sofia Davydycheva<sup>2</sup>, Tilman Hanstein<sup>2</sup>, Daniel Laudal<sup>3</sup>, Yardenia Martinez<sup>2</sup>, Kris MacLennan<sup>1</sup>, Shannon Mikula<sup>3</sup>, Don C. Adams<sup>1</sup>, Ryan J. Klapperich<sup>1</sup>, Wesley D. Peck<sup>1</sup>, and Kurt Strack<sup>2</sup>

<sup>1</sup>Energy & Environmental Research Center, University of North Dakota, USA

<sup>2</sup>KMS Technologies, USA

<sup>3</sup>Minnkota Power Cooperative, USA

### Summary

The North Dakota CarbonSAFE (Carbon Storage Assurance Facility Enterprise) project is part of the U.S. Department of Energy initiative to develop geologic storage sites to store 50+ million metric tons of carbon dioxide (CO<sub>2</sub>) from industrial sources. Geophysical methods are key for characterizing the geologic formations to store CO<sub>2</sub> and monitor the injected CO<sub>2</sub> over time to ensure containment. In the integrated multimeasurement geophysical approach considered for this project, it is expected that the controlled-source electromagnetic (CSEM) method is a strong contributor to mapping the CO<sub>2</sub> movement. A feasibility study of the CSEM method, including 1D and 3D modeling and a field noise test, was conducted to determine its effectiveness in monitoring CO<sub>2</sub> in the Broom Creek and Deadwood Formations. The study results demonstrate that the CSEM method can be used for CO<sub>2</sub> storage monitoring in the study area. Preliminary inversion results of magnetotelluric (MT) and CSEM field data confirm the quality of the anisotropic model developed in this study.

### Introduction

North Dakota CarbonSAFE is a multidisciplinary project that assesses safe, permanent, commercial-scale geologic storage of CO<sub>2</sub> generated by the Milton R. Young coal-fired power plant. The Energy & Environmental Research Center leads the project in partnership with the U.S. Department of Energy National Energy Technology Laboratory, Minnkota Power Cooperative, and BNI Energy. The study area is located near Center, North Dakota, with storage expected to be in the Broom Creek and Deadwood Formations at a depth of 1,700 and 3000 m, respectively.

The project's geophysical activities include borehole logging, 2D and 3D seismic, CSEM, MT, magnetics, and microgravity surveys. These data will be used in an integrated modeling/inversion approach to investigate their applicability for monitoring CO<sub>2</sub> plume location and conformance as an alternative to 3D seismic acquisition.

A vital part of the reservoir monitoring process is estimating the location and extent of the CO<sub>2</sub> front. Since CO<sub>2</sub> is resistive, electromagnetic (EM) methods such as the CSEM

method are well situated for monitoring CO<sub>2</sub> injected into a reservoir because of the strong conductivity contrast generated from CO<sub>2</sub> replacing brine or oil (Colombo et al., 2010; Zhdanov et al., 2013). In the case of CO<sub>2</sub> replacing brine, the reservoir's resistivity increases. When CO<sub>2</sub> replaces oil, the reservoir's resistivity decreases. The model sketch including the CSEM survey layout is shown in Fig. 1.

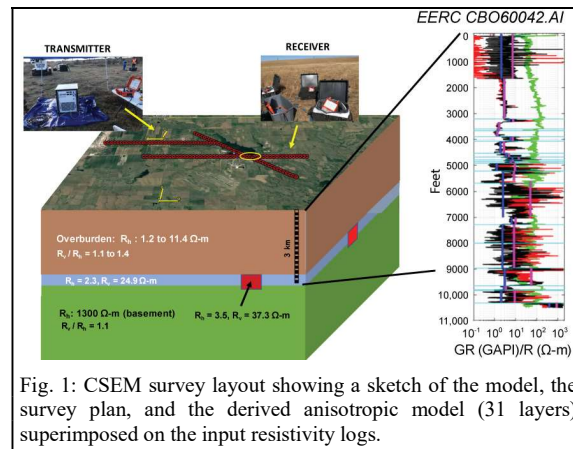


Fig. 1: CSEM survey layout showing a sketch of the model, the survey plan, and the derived anisotropic model (31 layers) superimposed on the input resistivity logs.

In this paper, a feasibility study to determine the CSEM method's effectiveness in monitoring CO<sub>2</sub> injected into the Broom Creek and Deadwood Formations after 1–2 years is presented. This study consisted of two parts: a 3D modeling of the CSEM response and a field noise test. The goal was to define the expected level of surface EM field response caused by an increase in CO<sub>2</sub> saturation and determine if signals of that magnitude could be detected in the field in the presence of observed noise levels. The result is an optimized survey design to minimize noise effects on the data. Although the ultimate proof will be the 3D time-lapse image from potential repeat surveys, the feasibility study's prediction can be verified with the initial field data by comparing the model derived from the logs with preliminary inversion results for the EM methods used in the project.

The integration of surface and borehole data is an essential requirement derived from 3D modeling. The data integration is achieved by measuring between surface-to-borehole and

## Using Controlled-Source Electromagnetic (CSEM) for CO<sub>2</sub> storage monitoring in the North Dakota CarbonSAFE Project

calibrating the information with conventional logs, and considering resistivity anisotropy (Strack, 2014). This process reduces the risk of imaging false anomalies (He et al., 2006 and 2010; Tietze et al., 2015; Thiel, 2016; Kalscheuer et al., 2018). Therefore, combining advances in acquisition hardware, imaging methods, 3D modeling, and workflow to integrate the surface models with borehole measurements in a CO<sub>2</sub> monitoring scenario is of paramount importance. In this scenario, high measurement accuracy and repeatability are required.

CSEM in the time domain is selected in this project because of its high sensitivity for onshore applications (e.g., Ceia et al., 2007; Strack and Aziz, 2013; Kumar and Hoversten, 2012). CSEM with grounded electric dipole excitation is better suited for reservoir analysis since the grounded transmitter excites both horizontal and vertical currents in the formation, making the method sensitive to thin anisotropic resistors. However, in CO<sub>2</sub> monitoring, sensitivity to both resistors and conductors is needed, namely, a full 3D anisotropic model. The MT method was used to measure the model's baseline background resistivity.

### Reservoir Monitoring Workflow

Once reservoir monitoring is required, a proper strategy to verify the monitoring results is needed as this process is long-term, and hardware, methods, and modeling codes evolve during this time frame (1–2 years). Thus borehole logs are taken as ground truth as they are on a reservoir scale and their limitations are well understood. Fig. 2 shows the CSEM reservoir monitoring workflow used here. The workflow's input data are interpreted as seismic horizons from a 3D prestack seismic cube, well logs with a maximum depth of 3000 m, which covered the depth of Deadwood Formation. The seismic horizons are predominantly flat and thus not shown. Using the deepest resistivity curve from the induction array 90" (Fig. 2, left), an anisotropic model was built based on algorithms for cumulative total electrical conductance and total cumulative resistance described in the literature (Keller and Frischknecht, 1967; Strack, 1992).

The total cumulative conductance (pink curve) and total cumulative resistance (black curve) are shown on the right of Fig. 3. The data are fit in sections interactively by a straight line. A fragmented line represents a layer boundary.

The equivalent resistivity or conductivity is calculated from the total data fitted by a line segment. In this process, the transverse resistance yields the vertical resistivity, and the cumulative conductance generates the horizontal resistivity. Both are end-member values, and all possible values and variations lie between them. A starting model with 31 layers and anisotropic resistivities results from this analysis (see Fig. 1, right). The derived layer boundaries mostly coincide

with seismic boundaries derived independently, which provides confidence in the derived model. In the next steps, the remaining logs are analyzed, and a fluid substitution (using Archie's equation) is carried out by replacing the brine with CO<sub>2</sub>. This 1D anisotropic model is used to build the 3D model considered in this project. In the workflow in Fig. 2, the two models lead to the parameter variation and, with the injection radius, the 3D model.

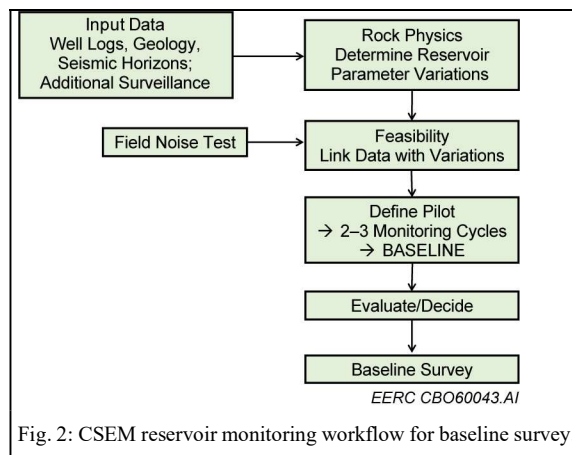


Fig. 2: CSEM reservoir monitoring workflow for baseline survey.

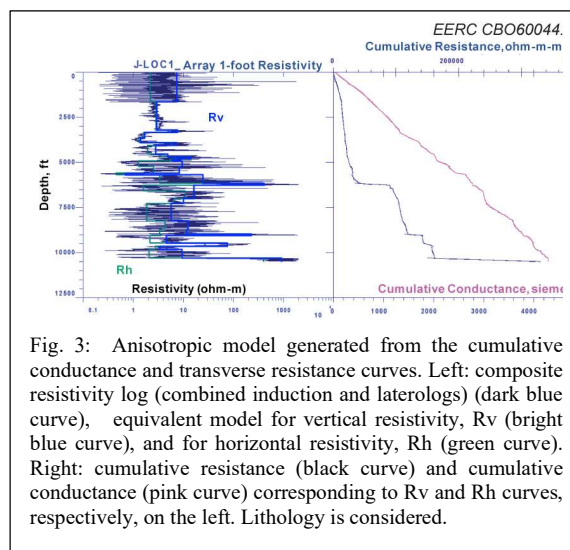


Fig. 3: Anisotropic model generated from the cumulative conductance and transverse resistance curves. Left: composite resistivity log (combined induction and laterologs) (dark blue curve), equivalent model for vertical resistivity, Rv (bright blue curve), and for horizontal resistivity, Rh (green curve). Right: cumulative resistance (black curve) and cumulative conductance (pink curve) corresponding to Rv and Rh curves, respectively, on the left. Lithology is considered.

### 3D Modeling

3D modeling is the core of the feasibility analysis (Davydycheva and Druskin, 1999). The following questions were addressed during the modeling activities for the study area:

## Using Controlled-Source Electromagnetic (CSEM) for CO<sub>2</sub> storage monitoring in the North Dakota CarbonSAFE Project

1. Can the changes in the data due to CO<sub>2</sub> injection be resolved in the presence of local noise?
2. What is the optimum receiver spacing for CSEM data acquisition?
3. Is it possible to image all of the reservoirs?

One transmitter and eight receivers along three-receiver lines were used to build various 3D models to answer the questions above. The receivers are at the injection well and represent the most distant receivers from Transmitter Location 1 (north location) and serve as a reference. The horizontal electric field response (Ex and Ey) and the vertical magnetic field as it changes with time (dBz/dt) are modeled.

The 3D modeling code was benchmarked against the 1D solutions for the same anisotropic model to understand electromagnetic field behavior regarding numerical noise and the noise caused by the modeling grid's approximation errors. These models are also used to estimate the optimum parameter range. This verification process allows separation of numerical accuracy limits, modeling artifacts, and anomalies caused by the model's features (e.g., very strong resistivity contrasts). The benchmark models covering most of the field scenarios are based on petrophysical analysis. Then the equipment/sensor choice is added to minimize the 3D modeling effort. The result is a set of models including the expected anomaly within the measurable time window.

First, 21 months of CO<sub>2</sub> injection in the Broom Creek Formation is simulated using a 60% average fluid saturation and an injection radius of 500 m. The simulation results demonstrated that 15–18 months of injection produced a sufficiently strong anomaly. Next, an injection radius of 150 m was used, and the required receiver spacing was estimated. Fig. 4 shows the 3D modeling results for the Broom Creek Formation for Ex, Ey, and dBz/dt for 100-, 200-, and 300-m receiver spacings. The reference noise from the noise test is shown at each component (horizontal dotted line). The response of all the components is above the noise level. The curve variations between the three spacing are smooth; therefore, the CO<sub>2</sub> anomaly can be reconstructed up to 300-m receiver spacing.

In the next step, as the Deadwood Formation has lower porosity and is significantly deeper than the other reservoir, a conservative 30% CO<sub>2</sub> saturation after injection (representing a 150-m flood zone radius) was considered. The Ex, Ey, and dBz/dt responses and difference corresponding to reservoir conditions before and after CO<sub>2</sub> injection are between 1% and 5% for 1D model and below 1% for 3D models. Monitoring injected CO<sub>2</sub> in the Deadwood Formation under the assumed field and survey parameters will be a challenge, and novel anomaly enhancing methods are needed.

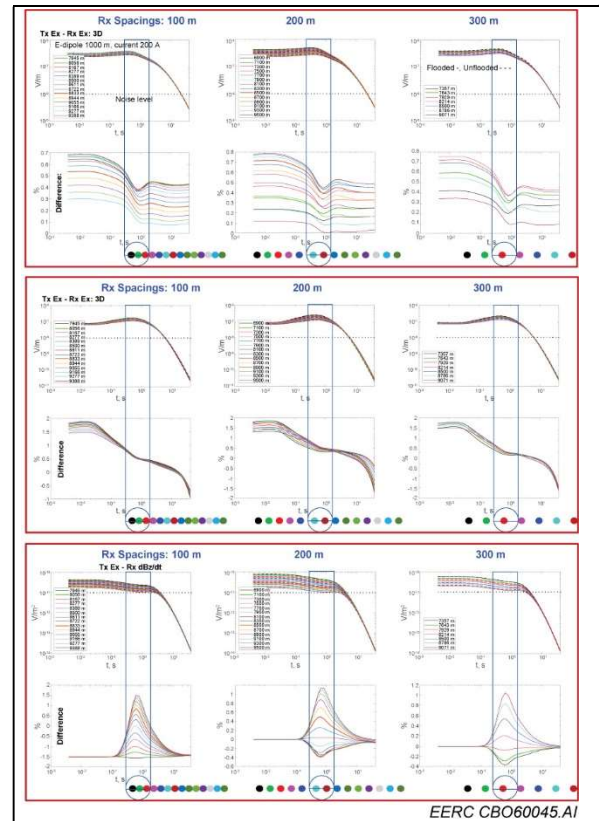


Fig. 4: Broom Creek 3D modeling results for 100 m (left), 200 m (middle), and 300 m (right) receiver spacings above the injection zone for the Ex receivers (top), Ey receivers (middle), and dBz/dt (bottom). The differences for each component are at the bottom. Data are displayed as a function of time. The transmitter is in the x-direction. Variations cover the offsets considered for this survey (curves of several colors) over the anomalous injection zone. Color dots in the bottom represent the receivers' map view above the injection zone using the same colors as the curves.

In designing a CSEM survey, the transmitter moment can increase by 3 to 5 times and the recording time by 4 to 16 hours, thus improving the signal-to-noise ratio (Strack, 1992). Alternatively, the focused source electromagnetic (FSEM) method (Davydycheva and Rykhlinski, 2009, 2011; Davydycheva, 2018) can be applied to improve the anomaly response by at least a factor of 10. Shallow (10 to 100 m) borehole receivers can also be considered to achieve similar strong responses as they measure the same vertical electric field. Therefore, all reservoirs can be imaged if the baseline survey is included to update imaging anomalies expected for FSEM to be between 1% and 5%.

# Using Controlled-Source Electromagnetic (CSEM) for CO<sub>2</sub> storage monitoring in the North Dakota CarbonSAFE Project

## Field Noise Test

Concurrent to the 3D modeling, field measurements were conducted in late 2020 to assess noise conditions. This allows optimization of the survey design and estimation of the data's signal-to-noise ratios. Magnetic field sensors (LEMI-120 induction coils and S20 air coils), electric sensors, and KMS-820 recording units were used in the test. An example of amplitude spectra of the CSEM and MT noise measurements is shown in Fig. 5. The amplitude of the noise recorded by the induction coils is higher than the air coil's noise. This difference suggests that the areal averaging of the air coil reduces some of the localized noise. 60-Hz noise and its harmonics observed in the raw data were attenuated as part of the data processing. Subsequently, the air coil data were used to simulate noise combined with the transmission cycle and signal processing. A CSEM transmitter's response is modeled for various transmitter-to-receiver offsets used in the field using the 31-layer anisotropic model (see Fig. 1). The analysis shown in Fig. 5 yields that the air coil is the best sensor and calculating RMS over the stacked duty cycle of the transmitter is a good noise-level estimator. Low-frequency amplitudes determine the noise level. The estimated optimum recording for CSEM data acquisition is 3:40 hours.

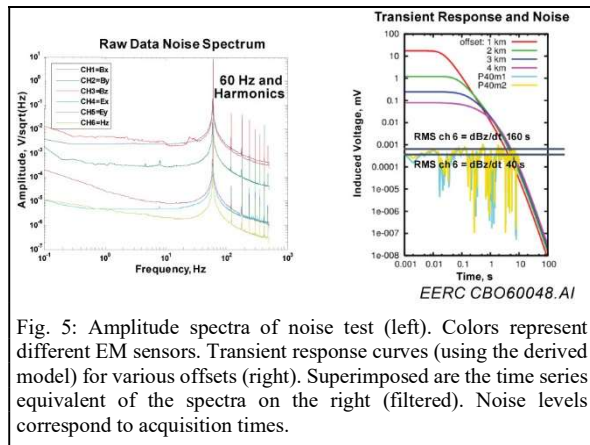


Fig. 5: Amplitude spectra of noise test (left). Colors represent different EM sensors. Transient response curves (using the derived model) for various offsets (right). Superimposed are the time series equivalent of the spectra on the right (filtered). Noise levels correspond to acquisition times.

The skin depth formula and the estimated lowest frequency at approximately 3000 m deep were used to derive the recording time for the MT data acquisition. The high frequency (HF) range includes power line noise and uses HF data processing, and the low frequency (LF) range is below the power line noise and uses LF data processing. This range is for overnight data acquisition. The variation of duration depends on when the station setup is finished and when the station is moved the next day.

## Conclusions

The feasibility study results demonstrate that the CSEM method can monitor injected CO<sub>2</sub> in the study area:

- Based on the noise analysis, changes in the resistivity data due to CO<sub>2</sub> injection can be resolved.
- It is feasible to use CSEM to image CO<sub>2</sub> injection in the Broom Creek Formation. Imaging the Deadwood Formation will be more challenging and requires additional feasibility data from the baseline survey to increase confidence.
- The optimum receiver spacing for the CSEM data acquisition is 200 to 300 m.
- The CSEM survey should be repeated after 18 months to monitor the reservoir fluid changes from CO<sub>2</sub> injection.

The background anisotropic resistivity model used in modeling was derived from combined deep resistivity logs. An example of the processing results for an average MT site with single and remote reference using the anisotropic model is shown in Fig. 6. The excellent results are proof of the model's appropriateness. The procedure to derive the background model was sufficient to obtain initial answers about the feasibility of using CSEM. However, monitoring the CO<sub>2</sub> saturation changes will require a more comprehensive background resistivity structure.

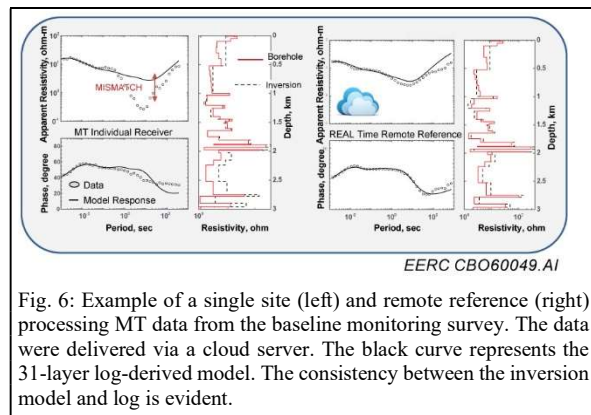


Fig. 6: Example of a single site (left) and remote reference (right) processing MT data from the baseline monitoring survey. The data were delivered via a cloud server. The black curve represents the 31-layer log-derived model. The consistency between the inversion model and log is evident.

## Acknowledgments

The authors would like to thank the U.S. Department of Energy National Energy Technology Laboratory for funding this work as part of Cooperative Agreement DE-FE0031889. The authors also thank Amanda J. Livers (EERC), Maxim Smirnov (KMS), A.Y. Paembonan (KMS), and Xiayu Xu (KMS). Without them, this work would not have been possible.

## REFERENCES

- Ceia, M. A., A. A. Carrasquilla, H. K. Sato, and O. Lima, 2007, Long offset transient electromagnetic (LOTEM) for monitoring fluid injection in petroleum reservoirs – Preliminary results of Fazenda Alvorada Field (Brazil): 10th International Congress of the Brazilian Geophysical Society & EXPOGEF 2007.
- Colombo, D., S. Dasgupta, K. M. Strack, and G. Yu, 2010, Feasibility study of surface-to-borehole CSEM for oil- water fluid substitution in Ghawar field, Saudi Arabia: AAPG GEO 2010 Middle East: Innovative Geoscience Solutions Meeting Hydrocarbon Demand in Changing Times.
- Davydycheva, S., 2018, Method and apparatus for detecting and mapping subsurface anomalies: U. S. Patent 9,891,339.
- Davydycheva, S., and V. Druskin, 1999, Staggered grid for Maxwell's equations in arbitrary 3-D inhomogeneous anisotropic media, in M. Oristaglio and B. Spies, eds., Three-dimensional electromagnetics: SEG, 119–137.
- Davydycheva, S., and N. Rykhlini, 2009, Focused source EM survey versus time-domain and frequency-domain CSEM: The Leading Edge, **28**, 944–949, doi: <https://doi.org/10.1190/1.3192841>.
- Davydycheva, S., and N. I. Rykhlini, 2011, Focused-source electromagnetic survey versus standard CSEM—3D modeling in complex, geometries: Geophysics, **76**, no. 1, F27–F41, doi: <https://doi.org/10.1190/1.3511353>.
- He, Z., W. Hu, and W. Dong, 2010, Petroleum electromagnetic prospecting advances and case studies in China: Surveys in Geophysics, **31**, 207–224, doi: <https://doi.org/10.1007/s10712-009-9093-z>.
- He, Z., X. Liu, W. Weiting, and H. Zhou, 2006, Mapping reservoir boundary by borehole-surface TFEM—Two case studies: The Leading Edge, **24**, 896–900, doi: <https://doi.org/10.1190/1.2056379>.
- Kalscheuer, T., N. Juhojuntti, and K. Vaitinen, 2018, Two-dimensional magnetotelluric modeling of ore deposits—Improvements in model constraints by inclusion of borehole measurements: Survey in Geophysics, **39**, 467–507, doi: <https://doi.org/10.1007/s10712-017-9454-y>.
- Keller, G. V., and F. C. Frischknecht, 1967, Electrical methods in geophysical prospecting: Pergamon Press.
- Kumar, D., and G. M. Hoversten, 2012, Geophysical model response in a shale gas: Geohorizons, **17**, 31–37.
- Strack, K. M., 1992, Exploration with deep transient electromagnetics: Elsevier, 373.
- Strack, K. M., 2014, Future directions of electromagnetic methods for hydrocarbon applications: Surveys in Geophysics, **35**, 157–177, doi: <https://doi.org/10.1007/s10712-013-9237-z>.
- Strack, K. M., and A. A. Aziz, 2013, Advances in electromagnetics for reservoir monitoring: Geohorizons, **18**, 32–44.
- Thiel, S., 2017, Electromagnetic monitoring of hydraulic fracturing—relationship to permeability, seismicity, and stress: Surveys in Geophysics, **38**, 1133–1169, doi: <https://doi.org/10.1007/s10712-017-9426-2>.
- Tietze, K., O. Ritter, and P. Veeken, 2015, Controlled source electromagnetic monitoring of reservoir oil saturation using a novel borehole-to-surface configuration: Geophysical Prospecting, **63**, 1468–1490, doi: <https://doi.org/10.1111/1365-2478.12322>.
- Zhdanov, M. S., M. Endo, N. Black, L. Spangler, S. Fairweather, A. Hibbs, G. A. Eiskamp, and R. Will, 2013, Electromagnetic monitoring of CO<sub>2</sub> sequestration in deep reservoirs: First Break, **31**, 71–78, doi: <https://doi.org/10.3997/1365-2397.31.2.66662>.